Indian Journal of Radio & Space Physics
Vol 50, December 2021, pp. 211-216

Particle-induced emission of X-rays from the Europa (100-10keV)

Smart Kundaserry Bright & C A Babu

Department of Atmospheric Sciences, Cochin University of Science and Technology, Kochi, Kerala 682 016, India

Received: 22 November 2021; Accepted: 30 November 2021

We considered the interaction of H^+, O^+ and S^+ ions of spectral energy range 100-10keV with the predominant H_2Oice composition of the surface of the Jovian Europa, and developed a model to quantify the ion-induced emission of X-rays from the satellite during its three encounters with Galileo mission flyby (E12, E19, E26). To achieve this, we computed the stopping power of H_2O ice using SRIM code, and X-ray ionization cross sections of interaction for the ions with H_2Oice using ISICS14 code. We found that the integrated fluxes of H^+, O^+ and S^+ ions are seen as lower above the current sheet (E19) and enhanced through the centre of the current sheet (E12) and below the current sheet (E26). The proton-induced energy flux received at the telescope of the Chandra X-ray Observatory (ergs-cm^{-2}-s^{-1}) during E12encounter is 9.49E-11, during E19encounter is 4.79E-11, and during E26encounter is 9.39E-11. The energy flux generated by O^+ and S^+ ions is found as trivial in comparison to the proton-induced energy flux (100-10 keV).

Keywords: Europa, Jovian, Magnetosphere, X-Rays, H_2O ice

1 Introduction

We focus in this paper on the particle-induced emission of X-rays from the Jovian Europa. The Europa, the smallest among the Galileans and the sixth-largest in the Solar System, sustain an atmosphere[1], an ionosphere[2], and is now regarded as an ocean satellite. The presence of an ocean is deducted from the perturbations aroused from the induced magnetic fields generated by the satellite in response to the recurring variation of the plasma in the Europan environment[3]. This salty liquid-water ocean of thickness 80-170kms[4] exist as a subsurface ocean sandwiched between a rocky interior, and an icy crust of thickness more than 3-4kms[5]. The H_2Oice, the predominant composition of the surface[6] favours the formation of an oxygen atmosphere, this molecular oxygen atmosphere has a surface pressure of 10^{-11}that of the Earth's atmosphere at sea level[7], and hence the atmosphere of the Europa is deemed as tenuous.

Being situated at $9.47R_J$ (radius of Jupiter, $R_J = 7.14 \times 10^4$km), the tenuous Europa resides wholly engulfed within the magnetosphere of its primary. The H^+, O^+ and S^+ ions predominantly populate the Jovian magnetosphere, the tenuous atmosphere of the Europa favours the direct interaction of these species with its surface, and the impinging charged-particles are known to induce particle-induced sputtering events at its surface[8] and elsewhere in the landscapes of the natural satellites of the Solar System. The energetics induced by these ions also results in particle induced emission of X-rays from its surface[9]. We considered in this context the interaction of H^+, O^+ and S^+ ions with the Europa, and quantified the subsequent particle-induced emission of X-rays from its surface. This is achieved by developing a numerical model under the following premises.

The interaction of energetic charged-particles with the regolith of the tenuous planetary objects causes ionization of the inner-shell electrons of its elemental composition. This scenario removes an electron from an atom of the target. Subsequently, the electrons from an outershell occupy the vacancy, and the loss of a specific amount of energy in this process in the case of radiative transitions appears as an X-ray photon. This process is known as particle-induced X-ray emission (PIXE). We developed in this context a model to compute the PIXE from the Europa by taking into account the probable mechanisms of particle-induced excitation of a target atom of the elemental constituent of its surface, the subsequent emission process of photons and computed the intensity of H^+, O^+ and S^+ ion induced emission of X-rays in the spectral energy range of 100 to 10keV from the surface of the Europa.

We present the theoretical formalism of the model used to compute the particle-induced emission of X-rays from the Europa and the composition of its surface used to model the X-ray emission. This work

Corresponding author (E-mail: babuca@cusat.ac.in)

considers the interaction of H^+, O^+ and S^+ ions with the H_2Oice. We discuss in this paper the irradiation fluxes of ions at the Europa distance influencing its surface energetics, cross sections of interactions for ions with oxygen in H_2O ice, stopping power of the H_2O ice medium for the impinging ions, the transmission of X-rays generated at different depths through theH_2O ice to the surface, the yield of the ion-induced emission of oxygen Kα X-rays from the H_2O ice, and the subsequent energy flux of X-rays (ergs-cm^{-2}-s^{-1}) received by the telescope of the Chandra X-ray Observatory.

2 Materials and Methods

We developed the theoretical formalism of the model by considering an incident charged-particle of mass M_1 of atomic number Z_1 of kinetic energy (E) of spectral energy range 100-10keV interacting with a target atom of mass M_2 and atomic number Z_2 of the medium. Subsequently, we considered in this work the interaction of protons (100-10keV) with oxygen in H_2Oice. The presence of H_2O on the surface of the Europa, deducted initially from the reduction in the intensity of the infrared (IR) spectra[10] beyond 1.5 μm (up to 2.5 μm) by a factor of 2-3, was later confirmed by the near-IR spectra (0.7-2.5 μm) obtained by Moroz et al.[11], who suggested that the records of the Europa show detail characteristic of the reflection spectrum of H_2O snow cover, and noted its wider presence in the surface. Model comparisons[12] found the H_2O ice in the surface as predominantly amorphous and the ice at ~1mm depth as predominantly crystalline.

All incident charged-particles interacting with the target medium has a certain probability of interaction with the constituents of the medium (1 barn = 10^{-24} cm^2), and this probability of interaction is expressed in terms of cross section. The X-ray ionization cross section$\sigma_i^Z(E)$is a measure of the vacancies, and; the X-ray production cross section$\sigma_p^Z(E)$ gives the effective transitions which end up with the emission of X-ray photons, and is obtained as a product of$\sigma_i^Z(E)$and the fluorescence yieldω_Z. The profiles of the charged-particles in the Jovian magnetosphere are obtained primarily from a model based on *in situ* data returned by the experiments on the Pioneer and the Voyager spacecraft[13]. The Galileo mission (launched on October18, 1989, 16:53:40 UTC) also observed the Jovian system until its forced decay (September 21, 2003, 18:57:00 UTC). We obtained the intensity profiles of the H^+, O^+ and S^+ ions in the vicinity of the Europa from the data measured by the Energetic Particle Detector (EPD) onboard the Galileo during multiple encounters which occurred near the centre of the current sheet (E12 encounter), above it (E19) and well below the current sheet (E26). The E12encounter was on 1997-3501216-1221UT (day 350 of 1997 from 1216-1221 UT) and thus occurred on December 16, 1997; E19 on February 1, 1999 (1999-0320201-0205 UT and 0225-0228 UT) and E26 on January 3, 2000 (2000-0031745-1750 UT).

We took the trajectory of the incident H^+, O^+, S^+ions as the X-direction, and computed the energy profile along this line using the stopping power of the H_2O ice medium [$S_M(E)$]. Stopping power conveys how much the particle loses energy at a certain distance when it travels in a medium. The parameter has a dependence on energy (E), mass (M_1) and atomic number (Z_1) of the particle and also on the mass (M_2), atomic number (Z_2) and density of the material (ρ_M) through which it passes. The electronic component of the stopping refers to the energy-loss of the particle due to the ionization or excitation of electrons of the medium resulting from the interaction of the incident particle with the target electrons of the constituents of the medium. When the particle has slowed down sufficiently, the collisions with nuclei become more probable and finally dominate the slowing down. The sum of the electronic [$dE(dx)_e^{-1}$] and the nuclear [$dE(dx)_n^{-1}$] stopping power provide the total stopping power of the medium [$dE(dx)^{-1}$].

If the energy of a particle changes an average of dE in a distance dx along its path, the linear stopping power (MeVcm^{-1}) defined as s=- [$dE(dx)^{-1}$] is written as a sum of the electronic and nuclear contributions. The stopping power defined by the density of the medium (ρ_M), known as its mass-stopping power $S_M(E)$, is a useful quantity because it expresses the rate of energy-loss of a particle per gcm^2 of the medium traversed (MeV-cm^2-g^{-1}), and is obtained by the division of s by ρ_M. We computed the depth penetrated in the H_2O ice by the charged-particle (R_{CSDA}) of an incident kinetic energy E_p while at a kinetic energy E under the approximation of the continuous slowing down of the particle (CSDA) in which the incident particle is regarded as losing its energy in a medium continuously at a rate equal to the total stopping power S_M (E) of the medium for the incident ions as:

$$R_{CSDA} = \int_0^{E_p} \frac{dE}{S_M(E)} \quad \ldots(1)$$

We derived the intensity profile of the ions driving the surface energetics on the Europa during E12, E19 and E26 encounters of the Galileo mission flybys with the satellite[14], computed the X-ray ionization cross sections (b) for protons of spectral energy range of 100-10keV interacting with the target oxygen atom in theH_2Oice medium using ISICS14[15], the stopping power of the H_2O ice (ρ=1.0gcm^{-3}) for H^+, O^+, S^+ ions (100-10keV) using SRIM[16] and the mass-attenuation coefficients for oxygen using the NIST-XCOM code[17].

Using the aforementioned parameters, and with the notations α and β as the generalized angles for the impact of the incident charged-particle and take off of X-rays, $\left(\frac{\mu}{\rho}\right)_{Z,\,M}$ as the concentration-weighted sum of the mass-attenuation coefficients of the elements of the medium, the effect of the attenuation coefficients on the X-ray intensity from an element of the path of the particle *en route* to the detector is obtained through the X-ray transmission factor T_Z (E), and we obtained the parameter using the eq. 2 of this work. The integration over all segments of the track of the particle then gives the total intensity of the yield of each Kα X-ray photon Y(Z) resulting from the passage of N_P particle through the medium (eq. 3) as:

$$T_Z(E) = exp\left[-\left(\frac{\mu}{\rho}\right)_{Z,M} \frac{cos\,(\alpha)}{sin\,(\beta)} \int_{E_p}^{E} \frac{dE}{S_M(E)}\right] \quad \ldots(2)$$

$$Y(Z) = \frac{C_Z}{A_Z} N_A N_p\, \omega_Z\, \frac{\Omega}{4\pi}\, \varepsilon_Z^i\, t_Z \int_{E_p}^{E_f} \frac{\sigma_i^Z(E)\, T_Z(E)}{S_M(E)}\, dE \quad \ldots(3)$$

Here, the notation C_Z pertain to the mass fraction of an element of the medium of atomic number Z of relative atomic mass A_Z (g mol^{-1}); N_A is the Avogadro's number (mol^{-1}), N_P is the number of the incident particles, and $\omega_{K,\,Z}$ is the fluorescence yield of the K-shell of an element having atomic number Z. For a particle of energy E, $\sigma_i^Z(E)$ is the X-ray ionization cross section (cm^2). The fractional solid angle subtended by the detector is denoted by $\Omega/4\pi$. The intrinsic efficiency of the detector is denoted by ε_Z^i, $t_{K,Z}$ is the transmission through any absorbers interposed between the medium and the detector, and we considered these parameters as of unit value. The notations E_p and E_f are the entry and exit energies of the particle, and when the medium is thick enough to stop it, we took E_f=0.

We later folded the X-ray yield of oxygen Kα X-ray photons from the H_2Oice for H^+, O^+, S^+ ions of spectral energy range of 100-10keV with the intensity profile of the ions during E12, E19 and E26encounter of Galileo mission flyby with the Europa, and scaled these numbers to the Europa as well as to the distance of the Chandra X-ray Observatory (CXO) to obtain the energy flux received at the telescope of the CXO (ergs-cm^{-2}-s^{-1}).

3 Results and Discussion

We considered the interaction of protons (M_1=1.008amu), O^+ion (M_1 =15.995 amu) and S^+ion (M_1=31.972 amu) of incident kinetic energy of 100-10keV with the H_2Oice (ρ=1.00 gcm^{-3}) of target density 3.09 × 10^{23}moleculescm^{-3} in which hydrogen have a mass percent of 11.19% and 88.81% for oxygen. We found that during E12encounter, the integrated proton flux in the Europan environment (ions/cm^2-s) is 6.84E+09, during E19 encounter is 3.21E+09, and during E26encounter is 7.00E+09 (Fig. 1). The integrated flux is seen as lower during E19 (3.21E+09) and enhanced through E12 (6.84E+09) and E26 (7.00E+09). We found that during E12 encounter, the integrated O^+ flux (ions/cm^2-s) is 3.90E+08, during E19 encounter is 3.44E+08, and during E26 encounter is 1.57E+09. The integrated flux is seen as lower during E19 (3.44E+08) and enhance through E12 (3.90E+08) and E26 (1.57E+09). We also found that during E12 encounter, the integrated flux of S^+ ion (ions/cm^2-s) is 8.64E+08, during E19 encounter is 9.19E+08, and during E26 encounter is 5.93E+09. The integrated flux is seen as lower during E12 (8.64E+08) and

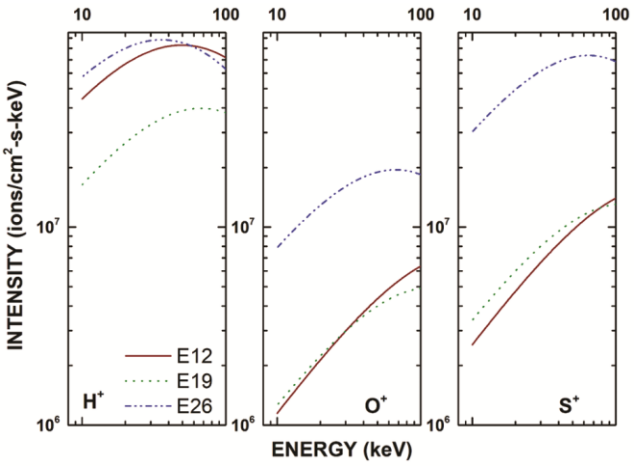

Fig. 1 — Panels present the profiles of the irradiation fluxes of H^+, O^+ and S^+ ions (ions/cm^2-s-keV) during E12 (near the centre of the current sheet), E19 (above the current sheet) and E26 (below the current sheet) encounter of Galileo mission flybys with the Europa.

enhanced through E19 (9.19E+08) and E26 (5.93E+09).

The X-ray ionization cross section (b) for a H^+ ion of incident kinetic energy of 100keV is found to be 12,605b, and this ion while at 10keV has an X-ray ionization cross section (b) of 0.355b. For O^+ ion of incident kinetic energy of 100keV, the cross section is 1.69E-07b and at 10keV is 1.587E-193b. For S^+ion of incident kinetic energy of 100keV, the cross section is 9.28E-38b, while at ~26.5keV is 2.099E-294b and at 10keV is 0. These numbers indicate that as the incident kinetic energy of an ion diminishes during its passage through the H_2O ice, the X-ray ionization cross section (b) is seen as diminishing (Fig. 2).

An incident H^+ion of kinetic energy 100keV interacting with the H_2Oice undergoes a diminishing of its incident energy within the medium. While it attains 10keV, we found that the ion can penetrate to a depth of 1.21 µm in the H_2O ice; an O^+ion to 0.48 µm and an S^+ion can reach a depth of 0.22 µm (Fig. 3). We also observed that an H^+ion of kinetic energy 20keV interacting with the H_2O ice medium while it attains 10keV can penetrate to a depth of 0.19 µm, an O^+ion to 52.25nm, and an S^+ion to 24.25nm. The Kα energy of oxygen is 0.5249keV, and the mass-attenuation coefficient of an oxygen photon is 2.656E+04cm^2/g. Taking into account the attenuation loss, we also calculated the transmission of oxygen Kα X-ray photons generated by the impinging ions from various depths of the H_2O ice to the surface (Table 1-3). We note that from a depth of 1.21 µm

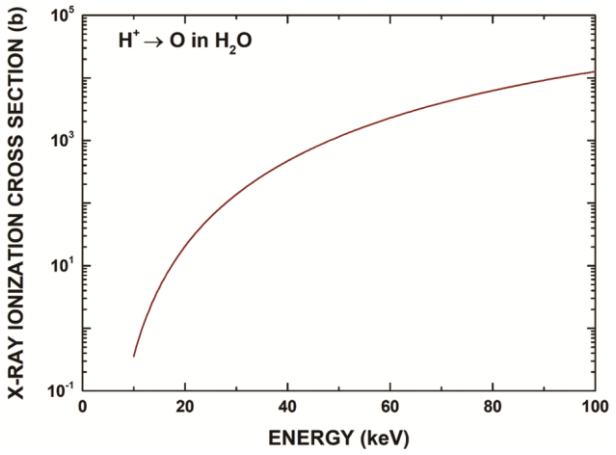

Fig. 2 — X-ray ionization cross section (b) for protons interacting with oxygen in the H_2O ice.

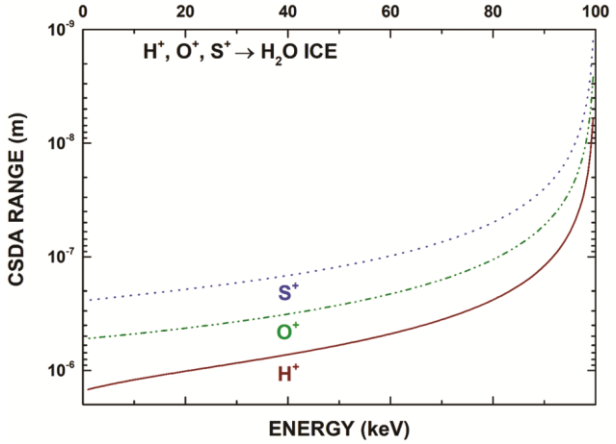

Fig. 3 — CSDA range (R_{CSDA}) against the incident kinetic energy E_p (100 keV) for the interaction of H^+, O^+ and S^+ ions with the H_2O ice surface composition model of the Europa's surface.

Table 1 — Depth of penetration of H^+ ion and transmission of X-rays from these depths.

Incident Energy of H^+ Ions (keV)	CSDA range (µm)	X-ray Transmission (%)
100	1.21	4.03
90	1.09	5.54
80	0.97	7.60
70	0.85	10.41
60	0.73	14.28
50	0.61	19.73
40	0.48	27.63
30	0.35	39.70
20	0.19	59.83

Table 2 — Depth of penetration of O^+ ion and transmission of X-rays from these depths.

Incident Energy of O^+ Ions (keV)	CSDA range	X-ray Transmission (%)
100	0.48 µm	28.19
90	0.42 µm	32.41
80	0.37 µm	37.30
70	0.32 µm	42.98
60	0.27 µm	49.54
50	0.21 µm	57.09
40	0.16 µm	65.75
30	0.11 µm	75.66
20	52.25 nm	87.04

Table 3 — Depth of penetration of S^+ ion and transmission of X-rays from these depths.

Incident Energy of S^+ Ions (keV)	CSDA range	X-ray Transmission (%)
100	0.22 µm	56.11
90	0.19 µm	59.96
80	0.17 µm	64.03
70	0.14 µm	68.31
60	0.12 µm	72.83
50	95.40 nm	77.62
40	71.60 nm	82.68
30	47.93 nm	88.05
20	24.25 nm	93.76

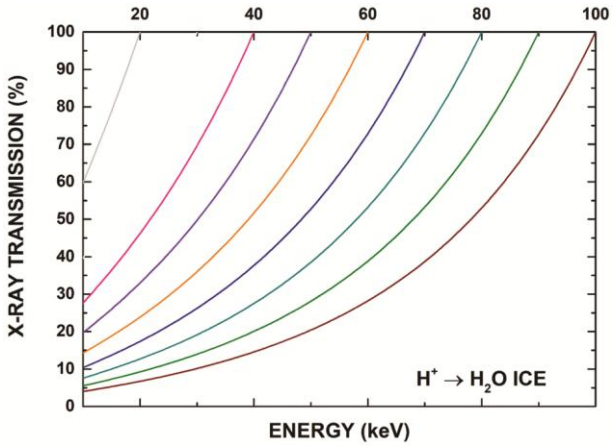

Fig. 4 — X-ray transmission to the surface for H^+ ions of incident kinetic energy of 100-10 keV while at 10 keV in the H_2O ice.

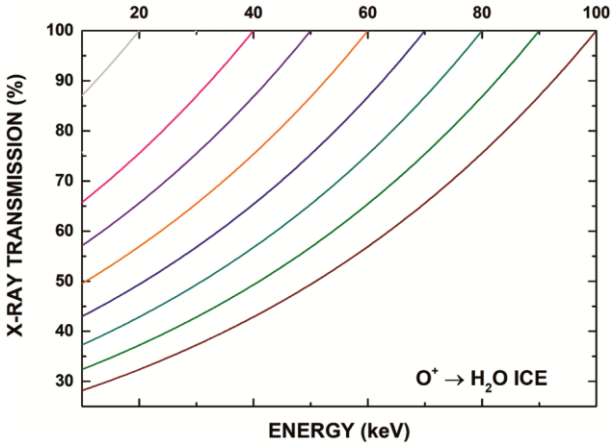

Fig. 5 — X-ray transmission to the surface for O^+ ions of incident kinetic energy of 100-10 keV while at 10 keV in the H_2O ice.

and 0.19 μm reached by a proton of 100keV and 20keV while at 10keV respectively, 4.03% (1.21 μm) and 59.83% (0.19 μm) of the X-rays generated at this depth can reach the surface of the satellite (Fig. 4). For O^+ (Fig. 5), the numbers for a 100keV ion while at 10keV is 0.48 μm (28.19%), and; for S^+ (Fig. 6), the numbers are 0.22 μm (56.11%).

These computations reveal that at both ends of the energy spectrum under consideration (100keV and 10keV), the ions that penetrate deeper in the H_2Oice are the H^+ions, and the depth of penetration diminish through O^+ ion and S^+ ion. This scenario reveals that the energetics induced by the protons of incident kinetic energy 100keV while at 10keV are spread within the medium over a depth of 1.21 μm, by the O^+ions to 0.48 μm and by the S^+ion to 0.22 μm. The numbers also indicate that the transmission of X-rays from a depth is seen as maximum for the ions of

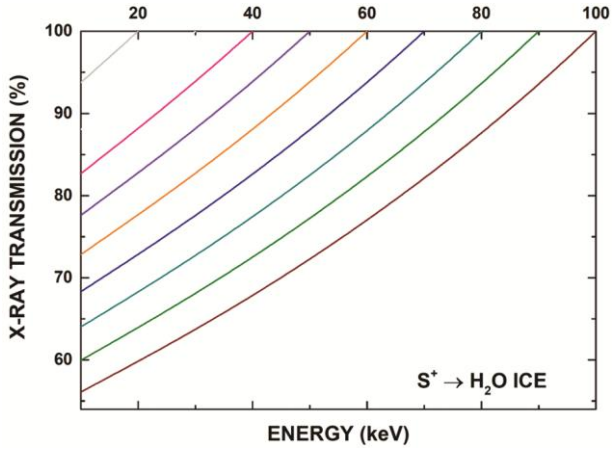

Fig. 6 — X-ray transmission to the surface for S^+ ions of incident kinetic energy of 100-10 keV while at 10 keV in the H_2O ice.

lower energy (10keV) than energetic ions (100keV). The energetic ions penetrate deeper, and the photons generated at greater depths are seen as undergoing a higher attenuation than the ions that penetrate shallower depths.

We found that the protons of incident kinetic energy 100-10keV can generate an X-ray yield of 104.18 oxygen Kα photons from the H_2Oice medium. Due to the negligible range of cross sections, the X-ray yield generated by the O^+ions and S^+ions are seen as nil. The proton-induced energy flux received at the telescope of the Chandra X-ray Observatory during E12 encounter (December 16, 1997) is 9.49E-11 ergs-cm^{-2}-s^{-1}, during E19encounter (February 1, 1999) is 4.79E-11 ergs-cm^{-2}-s^{-1}, and during E26 encounter (January 3, 2000) is 9.39E-11 ergs-cm^{-2}-s^{-1}.

4 Conclusion

The integrated fluxes of H^+, O^+ and S^+ions in the Europan environment is seen as lower above the current sheet (E19) and enhanced through the centre of the current sheet (E12) and below the current sheet (E26). The X-ray ionization cross section (b) for H^+ion is seen as of relatively higher magnitude than of O^+ and S^+ions. H^+ion penetrates deeper than O^+ and S^+, and an H^+ion of incident kinetic energy of 100keV while at 10keV can travel to a distance of 1.21 μm, O^+ to 0.48 μm and S^+ to 0.22 μm. From these depths, 4.03%, 28.19% and 56.11% of oxygen Kα X-ray photons can reach the surface. The proton-induced X-ray energy flux received at the telescope of the Chandra X-ray Observatory (CXO) is found as varying from 4.79E-11 to 9.49E-11 ergs-cm^{-2}-s^{-1}.

Acknowledgement

Smart K. B., one of the authors, was supported for this work by the university fellowship through Cochin University of Science and Technology (CUSAT).

References

1 Hall, D T, Strobel, D F, Feldman, P D, McGrath, M A, & Weaver, H A, Nature, 373 (1995) 677.
2 Kliore, A J, Science, 277 (1997) 355.
3 Khurana, K K, Kivelson, M G, Stevenson, D J, Schubert, G, Russell, C T, Walker, R J, & Polanskey, C, Nature, 395 (1998) 777.
4 Anderson, J D, Schubert, G, Jacobson, R. A, Lau, E L, Moore, W B, & Sjogren, W L, Science, 281, (1998) 2019.
5 Turtle, E P, & Pierazzo, E, Science, 294, (2001) 1326.
6 Clark, R N, J Geophys Res: Solid Earth, 86 (1981) 3087.
7 Hall, D T, Strobel, D F, Feldman, P D, McGrath, M A, & Weaver, H A, Nature, 373 (1995) 677.
8 Lanzerotti, L J, Brown, W L, Poate, J M, & Augustyniak, W M, Geophys Res Lett, 5, (1978) 155.
9 Bhardwaj, A, Lisse, C M, & Dennerl, K, Encyclopedia of the solar system (3rd ed.), edited by T. Spohn, D. Breuer, & T. V. Johnson (Elsevier Science Publishing), 2014, 1019.
10 Kuiper, G P, Astron J, 62 (1957) 245.
11 Moroz, V I, Sov Astron, 9 (1966) 999.
12 Hansen, G B, & McCord, T B, J Geophys Res: Planets, 109 (2004) E01012.
13 Divine, N, & Garrett, H B, J Geophys Res: Space Phys, 88 (1983) 6889.
14 Paranicas, C, Ratliff, J M, Mauk, B H, Cohen, C, & Johnson, R E, Geophys Res Lett, 29 (2002) 18-1.
15 Liu, Z, & Cipolla, S J, Comput Phys Commun, 97 (1996) 315.
16 Ziegler, J F, *The Stopping and Range of Ions in Solids*, Pergamon, United States (1985).
17 Berger, M J, & Hubbell, J H, NBSIR, (1987) 87-3597.